

Thermal conductivity of porous structures

L. Braginsky,* V. Shklover, and G. Witz

Laboratory of Crystallography, ETH Zürich, 8093 Zürich, Switzerland

H.-P. Bossmann

Alstom (Schweiz) AG, Brown Boveri Strasse 7, 5401 Baden, Switzerland

(Received 21 July 2006; revised manuscript received 24 December 2006; published 12 March 2007)

Thermal conductivity of porous media is considered. The model permits regular power-series expansion of the expression for thermal conductivity as a function of porosity. The coefficients of the expansion depend on two-site correlation function of local thermal conductivities, which can be calculated from the microscopy image of the structure. Thermal conductivities of some model two-dimensional structures as well as a real porous yttria-stabilized zirconia film are calculated and discussed.

DOI: [10.1103/PhysRevB.75.094301](https://doi.org/10.1103/PhysRevB.75.094301)

PACS number(s): 66.70.+f, 44.30.+v, 44.05.+e, 05.60.-k

I. INTRODUCTION

The problem of heat transport in porous solid films attracts much attention of researchers due to their possible application as thermal barrier coatings. First of all, this concerns yttrium-stabilized ZrO₂ (YSZ), in which its thermal conductivity at 1000 °C is about 2 W/m K and can be reduced by microstructure modification. Meanwhile, some other materials of low thermal conductivity (TC) draw attention: Y₃Al₅O₁₂, nanocrystalline Al₂O₃ and superlattices W/Al₂O₃,¹ and multicomponent oxides, e.g., ZrO₂-(Y, Gd, Yb)₂O₃.²

There are two ways of heat transport in solid dielectrics at high temperatures: the phononic and radiation mechanisms of thermal conductivity. The former is due to the lattice vibration, whereas the latter is due to excitation and propagation of infrared light in a heated solid. The radiation component is significant at high temperatures only ($T \gtrsim 1000$ °C). In the case of low electron-phonon interaction, $\kappa = \kappa_{ph} + \kappa_r$, where κ is the total thermal conductivity and κ_{ph} and κ_r are its phononic and radiation components, respectively.³ This permits us to consider each component of thermal conductivity independently.

Aside from phononic and radiation mechanisms, there are some other contributions to the thermal conductivity. First of all, this concerns electronic component of thermal conductivity that dominates in metals. For YSZ at high temperatures (above 300 °C), similar component arises due to drift of O²⁻ ions.⁴ The mean free path of phonons as well as electrons in metals and O²⁻ ions in YSZ is much less than the pore size. This allows us to add all these nonradiation contributions to the thermal conductivity, so that $\kappa = \kappa_{nr} + \kappa_r$, where κ_{nr} is the sum of all nonradiation components of thermal conductivity essential for the material under consideration.

In this study, we deal only with the nonradiation component of thermal conductivity. The simple model we adopt neglects heat transport through the pores. It is commonly accepted that thermal conductivity of the porous solids can be expressed as $\kappa_{nr} = \kappa_i \Phi(p)$, where κ_i is the thermal conductivity of the appropriate dense material and Φ is the factor determined by porosity p . We shall call Φ the porosity factor. Different authors have proposed different estimations for its

value. Klemens⁵ used a thermodynamical approach to investigate heat propagation in porous solids. He shows that the thermal conductivity of the isotropic porous media with small volume fraction of pores (low porosity) is $\kappa_{nr} = \kappa_i(1 - 4p/3)$. This result is justified in experiments.⁶

Shafiro and Kachanov⁷ and Sevastianov and Kachanov⁸ studied the influence of the nonspherical (elliptical) pores and cracks on thermal conductivity. The result is $\kappa_{nr} = \kappa_i(1 - 8\varrho/9)$, where ϱ is the so-called crack density parameter; this parameter has been introduced to determine the influence of the nonspherical inclusions.⁷ For the particular case of spherical pores, this approximation yields $\kappa_{nr} = \kappa_i(1 - 3p/2)$. The model of Ref. 7 has been generalized in Ref. 8 to consider the large number of anisotropically distributed cracks; the single parameter describing the crack anisotropy has been suggested.

Wang *et al.*⁹ proposed to use the microscopy image of porous structure to calculate its thermal conductivity. The model includes the image analysis, which is necessary to develop the model structure comprising the pores, cracks, and voids of different sizes. This model structure has been used then for the direct calculation of thermal conductivity with the finite element method. The approach allows one to obtain a detailed map of the temperature field and the heat flux distribution. However, consideration of a large structure containing too many pores and cracks of different sizes seems to be difficult because of computational complexity.

In this paper, we suggest another approach of using the microscopy image of a porous structure to calculate its thermal conductivity. We proved that the effective thermal conductivity of porous media can be expressed via the pairing correlation function of local thermal conductivities taken in different points. This value can be easily calculated from the microscopy image. Corson¹⁰ and Berryman¹¹ developed technical details of such a procedure. We suggest the diagrammatic technique, similar to that used in particle and statistical physics for estimation of average amplitudes,¹³ to develop the thermal conductivity as series of porosity. We show that the expression^{5,6} $\kappa_{nr} = \kappa_i(1 - 4p/3)$ holds for the thermal conductivity of the isotropic porous media of low porosity in the absence of interaction between the pores and propose an improvement to take this interaction into account.

We consider the effect of large pores, the size of which is $0.1 \mu\text{m}$ or larger, which are typical for YSZ, on the thermal conductivity. The wavelength of the phonon responsible for the heat transport at high temperatures is of about a lattice constant (a few tens of angstroms), and the mean free path of such phonons is about 100 nm or less.¹⁴ This means that pores whose size exceeds $0.1 \mu\text{m}$ can be considered as large. To take them into account, we write the heat-flow equation with the position dependent thermal-conductivity coefficient.

II. MODEL

A. Effective thermal conductivity

To define this notion, it is useful to introduce some effective homogeneous, in general, anisotropic media, the response of which on the external heating is equal to that of the porous media under consideration. The thermal conductivity of this effective media will be identified with the effective thermal conductivity of the porous media. Let us begin with this effective media and suppose that momentary heating takes place at some point which we assume to be the coordinate origin. We are interested in the evolution of temperature at some remote point \mathbf{L} . We suppose that the distance $|\mathbf{L}|$ between this point and the coordinate origin considerably exceeds any other characteristic size of the problem. The temperature T obeys the heat-flow equation

$$\frac{\partial T}{\partial t} - \kappa_{ij} \frac{\partial^2 T}{\partial x_i \partial x_j} = \delta(\mathbf{r}, t), \quad (1)$$

which can be solved by means of Fourier transform

$$T(\mathbf{r}, t) = \frac{1}{(2\pi)^4} \int \theta(\mathbf{q}, \omega) e^{i(q_i x_i - \omega t)} d^3 q d\omega,$$

where $\theta(\mathbf{q}, \omega)$ is the Fourier transform of temperature, \mathbf{q} and ω are the relevant wave vector and frequency, respectively. Then,

$$\theta(\mathbf{q}, \omega) = \frac{1}{\kappa_{ij} q_i q_j - i\omega}, \quad (2)$$

so that

$$T(\mathbf{r}, t) = \frac{1}{(2\pi)^4} \int \frac{e^{i(q_i x_i - \omega t)}}{\kappa_{ij} q_i q_j - i\omega} d^3 q d\omega. \quad (3)$$

In particular, for an isotropic media where $\kappa_{ij} = \kappa \delta_{ij}$, this leads to the well-known result

$$T(\mathbf{r}, t) = \frac{1}{8(\pi \kappa^2 t)^{3/2}} e^{-|\mathbf{r}|^2/4\kappa^2 t}.$$

Consider now a similar problem for the porous material. We call $\bar{\kappa}_{ij}$ the effective thermal conductivity of the porous media, if this value permits us to estimate the average temperature at a remote point from Eqs. (2) and (3) by the substitution $\kappa_{ij} = \bar{\kappa}_{ij}$. This means also that the average temperature obeys the heat-flow equation with $\bar{\kappa}_{ij}$ as the thermal conductivity. Apparently, this notion is reasonable if $\bar{\kappa}_{ij}$ is independent of the distance $|\mathbf{L}|$. We shall show this in Sec. II C.

B. Description of porous media: Correlation function

If the size of pores much exceeds all mean free paths essential for the heat transport, then the temperature T obeys the heat-flow equation with the position dependent thermal-conductivity coefficient $\kappa(\mathbf{r})$:

$$\frac{\partial T}{\partial t} - \text{div}[\kappa(\mathbf{r}) \text{grad } T] = \delta(\mathbf{r}, t), \quad (4)$$

where

$$\kappa(\mathbf{r}) = \begin{cases} \kappa_i & \text{outside the pores} \\ 0 & \text{inside the pores.} \end{cases}$$

We can write the thermal-conductivity coefficient as the sum of its average κ_0 and fluctuate $\eta(\mathbf{r})$ components as follows:

$$\kappa(\mathbf{r}) = \kappa_0 + \eta(\mathbf{r}),$$

where

$$\kappa_0 = \kappa_i(1-p), \quad \overline{\eta(\mathbf{r})} = 0.$$

κ_i is the intrinsic thermal conductivity of the material under consideration, and p is the porosity.¹⁵ Perturbation with respect to $\eta(\mathbf{r})$ permits us to study the effect of disorder in terms of the two-point correlation function (CF) $S(\mathbf{r}, \mathbf{r}') = \overline{\eta(\mathbf{r}) \eta(\mathbf{r}')}$. For a homogeneous, in average, porous media,¹⁶ this value depends only on the distance, $S(\mathbf{r}, \mathbf{r}') = S(\mathbf{r} - \mathbf{r}')$. This function is maximal at zero, $S(0) = \overline{\eta^2(\mathbf{r})} = p(1-p)\kappa_i^2$, and vanishes at infinity: because fluctuations $\eta(\mathbf{r})$ and $\eta(\mathbf{r}')$ are independent, then $|\mathbf{r} - \mathbf{r}'| \rightarrow \infty$. Further, we will use the normalized correlation function $W(\mathbf{r} - \mathbf{r}') = S(\mathbf{r} - \mathbf{r}')/S(0)$; this function is independent of the conductivity κ_i and determined only by the structure of the pore media.

The attenuation length of the correlation function is comparable with the mean pore size R . Note that this size can be different in different directions for the anisotropic pores, e.g., cracks. Additional peculiarities of the correlation function are due to interaction (interconnection) of pores, which is small for low porosity. Generally speaking, the correlation function $W(\mathbf{r} - \mathbf{r}')$ can be calculated from the microscopy image, if it allows reconstruction of the three-dimensional (3D) image of porous media.

The four-point and other multipoint correlations, which arise from the higher orders of the perturbation, can be decomposed into two-point ones: $\overline{\eta(\mathbf{r}_1) \eta(\mathbf{r}_2) \eta(\mathbf{r}_3) \eta(\mathbf{r}_4)} = \overline{\eta(\mathbf{r}_1) \eta(\mathbf{r}_2)} \cdot \overline{\eta(\mathbf{r}_3) \eta(\mathbf{r}_4)} + \overline{\eta(\mathbf{r}_1) \eta(\mathbf{r}_3)} \cdot \overline{\eta(\mathbf{r}_2) \eta(\mathbf{r}_4)} + \overline{\eta(\mathbf{r}_1) \eta(\mathbf{r}_4)} \cdot \overline{\eta(\mathbf{r}_2) \eta(\mathbf{r}_3)}$. Corrections to this equality is appreciable, only if all relevant points are close, $|\mathbf{r}_1 - \mathbf{r}_2| \sim |\mathbf{r}_1 - \mathbf{r}_3| \sim |\mathbf{r}_1 - \mathbf{r}_4| \sim R$. They can be omitted in thermal-conductivity evaluation, if the mean size of pores is less than the size of the specimen.

C. Determination of effective thermal conductivity

The Fourier transform of the temperature $\Theta(\mathbf{k}, \omega)$ can be introduced as

$$T(\mathbf{r}, t) = \frac{1}{(2\pi)^4} \int \Theta(\mathbf{k}, \omega) e^{i(\mathbf{k}\mathbf{r} - \omega t)} d^3k d\omega.$$

By substituting this into Eq. (4), multiplying by $e^{-i\mathbf{q}\mathbf{r}}$, and integrating over the entire space, we find the equation for $\Theta(\mathbf{k}, \omega)$,

$$(\kappa_0 q^2 - i\omega)\Theta(\mathbf{q}, \omega) + \frac{1}{(2\pi)^3} \int \mathbf{k}\mathbf{q} \tilde{\eta}(\mathbf{k} - \mathbf{q}) \Theta(\mathbf{k}, \omega) d^3k = 1, \quad (5)$$

where

$$\tilde{\eta}(\mathbf{k}) = \int \eta(\mathbf{r}) e^{i\mathbf{k}\mathbf{r}} d^3r$$

is the Fourier transform of η .

The solution of Eq. (5) can be developed as series in $\tilde{\eta}$:

$$\Theta = \Theta_0 + \Theta_1 + \Theta_2 + \dots, \quad (6)$$

where

$$\begin{aligned} \Theta_0(\mathbf{q}) &= \frac{1}{\kappa_0 q^2 - i\omega}, \\ \Theta_1(\mathbf{q}) &= -\frac{\Theta_0}{(2\pi)^3} \int \mathbf{k}\mathbf{q} \tilde{\eta}(\mathbf{k} - \mathbf{q}) \Theta_0(\mathbf{k}) d^3k, \\ &\dots \\ \Theta_n(\mathbf{q}) &= -\frac{\Theta_0}{(2\pi)^3} \int \mathbf{k}\mathbf{q} \tilde{\eta}(\mathbf{k} - \mathbf{q}) \Theta_{n-1}(\mathbf{k}) d^3k. \end{aligned} \quad (7)$$

This series is presented graphically in Fig. 1, where straight lines correspond to $\Theta_0(\mathbf{k})$ and crosses to the factors $-(2\pi)^{-6} \mathbf{k}_1 \mathbf{k}_2 \tilde{\eta}(\mathbf{k}_1 - \mathbf{k}_2)$. Integration over \mathbf{k}_1 , \mathbf{k}_2 , etc., is assumed.

To determine the average temperature in disordered porous media, we have to average each term of the equation in Fig. 1 over the random value $\tilde{\eta}$. Then, the terms odd on $\tilde{\eta}$ vanish. As to the rest, we can evaluate them as sums of paired averages, as it is presented in Fig. 2. See Appendix A for the details of calculations.

In Fig. 2, the thin straight lines correspond to Θ_0 [Eq. (7)], the bold straight lines to the total sum Θ [Eq. (6)], and the dashed lines to Fourier transforms of the correlation function,

$$\tilde{W}(\mathbf{k}) = \int W(\mathbf{r}) e^{i\mathbf{k}\mathbf{r}} d^3r,$$

and the factor $\kappa_i[\mathbf{q} \cdot (\mathbf{q} - \mathbf{k})]$ corresponds to each vertex between $\Theta_0(\mathbf{q})$, $\Theta_0(\mathbf{q} - \mathbf{k})$, and $\tilde{W}(\mathbf{k})$. Integration over the inner \mathbf{k} vectors [i.e., $d^3k/(2\pi)^3$] is assumed. The total wave vector ($\Sigma \mathbf{k}$) obeys the conservation law at each vertex. This law

$$\overline{\mathbf{q}} = \overline{\mathbf{q}} + \overline{\mathbf{q} \times \mathbf{k}} + \overline{\mathbf{q} \times \mathbf{k}_1 \times \mathbf{k}_2} + \dots$$

FIG. 1. Solution of Eq. (5).

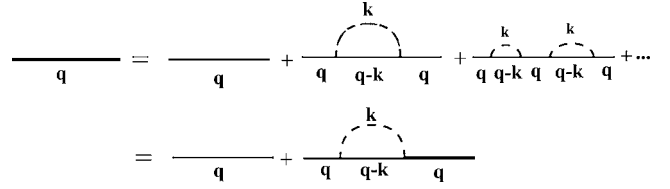


FIG. 2. Average temperature in the first approximation on p .

permits addition of diagrams in Fig. 2. The result is

$$\Theta = \frac{1}{(\kappa_0 - \Sigma) q^2 - i\omega}, \quad (8)$$

where

$$\Sigma = \frac{\kappa_i^2 p(1-p)}{(2\pi)^3} \int \frac{k_z^2 \tilde{W}(\mathbf{k} - \mathbf{q})}{\kappa_0 k^2 - i\omega} d^3k.$$

The typical value of q_i in Eq. (3) is $q \sim 1/L \rightarrow 0$, $\omega \sim \kappa^2/L^2 \rightarrow 0$, whereas $|\mathbf{k}| \sim 1/R$, where R is the mean pore size. This allows us to assume $|\mathbf{q}| \ll |\mathbf{k}|$, $\omega \rightarrow 0$, and omit these values in all the lines except the incoming and outgoing. Then, Σ becomes independent of q and ω . For the cubic symmetry of the correlation function, $\Sigma = (1/3) \kappa_i^2 \kappa_0^{-1} p(1-p) \times (2\pi)^{-3} \int \tilde{W}(\mathbf{k}) d^3k = p\kappa_i/3$; thus¹⁷

$$\bar{\kappa} = \kappa_i \left(1 - \frac{4}{3} p \right). \quad (9)$$

This coincides with the result of Refs. 5 and 6.

The second-order corrections that have not been considered in Fig. 2 correspond to the diagrams in Fig. 3. To take into account the first diagram, we have to replace the thin $\Theta_0(\mathbf{k})$ line in Fig. 2 with the bold one, i.e., to substitute $\Theta(\mathbf{k})$ for $\Theta_0(\mathbf{k})$. This leads to

$$\Sigma = \frac{\kappa_i}{2} \left[1 - p \sqrt{1 - \frac{10}{3} p + \frac{7}{3} p^2} \right]$$

and

$$\bar{\kappa} \approx \kappa_i \left(1 - \frac{4}{3} p - \frac{1}{9} p^2 \right).$$

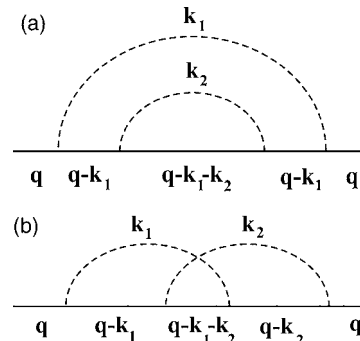


FIG. 3. Second-order (p^2) corrections to the diagrams of Fig. 2.

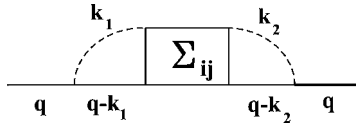


FIG. 4. General form of correction to the diagrams of Fig. 2.

The second diagram yields the tensor correction to the effective thermal conductivity. It can be written as $q_i q_j \Sigma_{ij}$, where

$$\Sigma_{ij} = \frac{\kappa_i^4 p^2 (1-p)^2}{(2\pi)^6 \kappa_0^3} \int \frac{k_1 k_2 j [k_1 \cdot (k_1 + k_2)] [k_2 \cdot (k_1 + k_2)]}{k_1^2 k_2^2 (k_1 + k_2)^2} \times \tilde{W}(k_1) \tilde{W}(k_2) d^3 k_1 d^3 k_2. \quad (10)$$

The symmetry of this tensor is determined by the symmetry of the correlation function $\tilde{W}(k)$. Supposing the cylindrical symmetry, the z axis of which is directed along the normal to the coating, we can assume $\tilde{W}(k)$ to be independent of the coordinate angles. Integrating with regard to these angles

shows that Σ_{ij} is the diagonal tensor and $\Sigma_{xx} = \Sigma_{yy} \neq \Sigma_{zz}$. For the spherical symmetry, $\Sigma_{xx} = \Sigma_{yy} = \Sigma_{zz}$.

In general, the total correction to the effective thermal conductivity can be presented with the diagram in Fig. 4. Here, Σ_{ij} is the sum of the terms of Fig. 2, Fig. 3, and others, which come from higher orders on porosity. It is important that Σ_{ij} is independent of q for $R \ll L$; this permits us to consider $\kappa_{ij} = \kappa_0 - \Sigma_{ij}$ as the effective thermal conductivity of the porous media.

III. SOME SIMPLE TWO-DIMENSIONAL MODELS

Let us estimate effective thermal conductivity [or, more precisely, the porosity factor $\Phi(p)$] of the model two-dimensional (2D) structures presented in Fig. 5. The structure in Fig. 5(a) represents a material with spherical pores of the same size, whereas materials shown in Figs. 5(b) and 5(c) have elliptical pores (cracks) (with aspect ratio 1:4) of the same (b) or different (c) orientations with regard to the substrate. It is important that the direction along the longer axis of the ellipses is particular in Fig. 5(b); meanwhile, the structures in Figs. 5(a) and 5(c) have no particular direction.

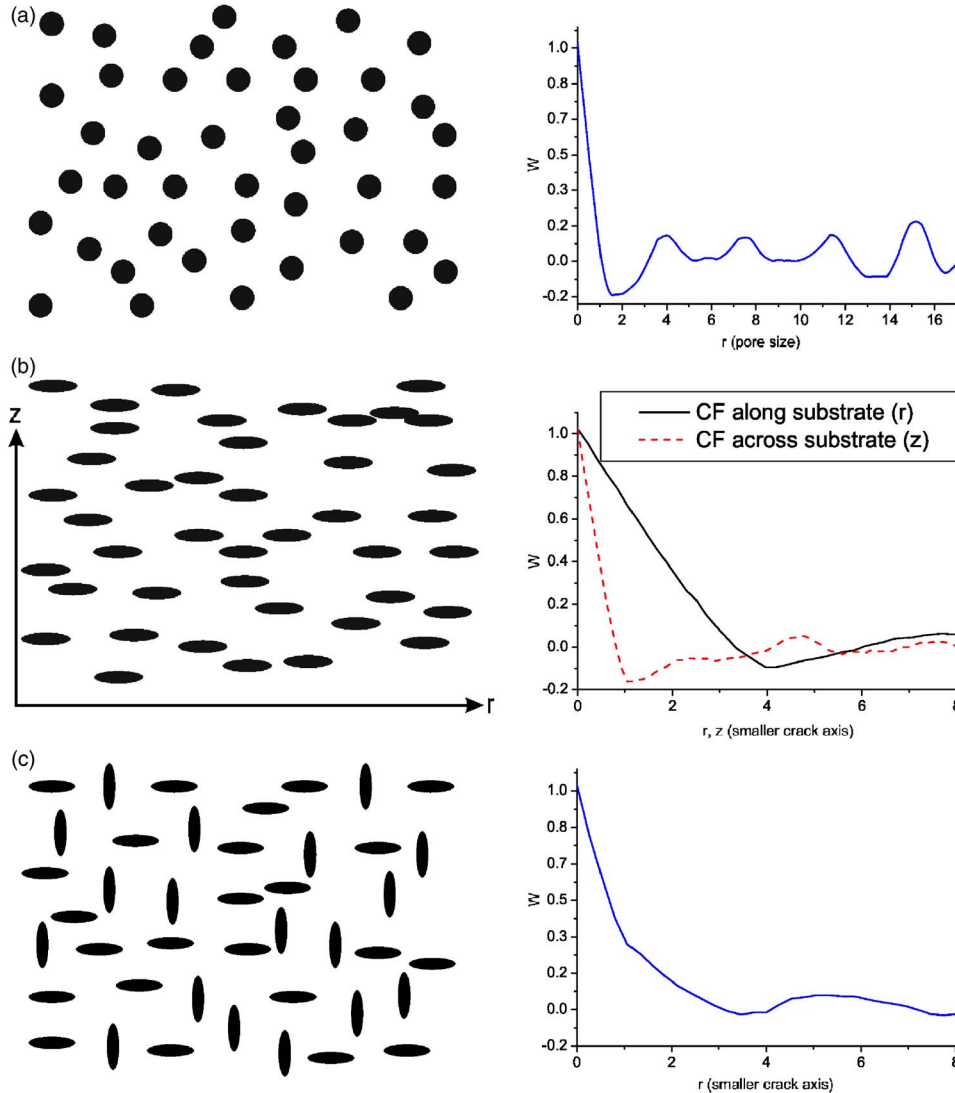


FIG. 5. (Color online) Two-dimensional models of pore structures (left) used in the calculations and the corresponding correlation functions vs distance (right). Characteristic pore size is used as the unit of distance. Aspect ratio of the ellipses in (b) and (c) is 1:4.

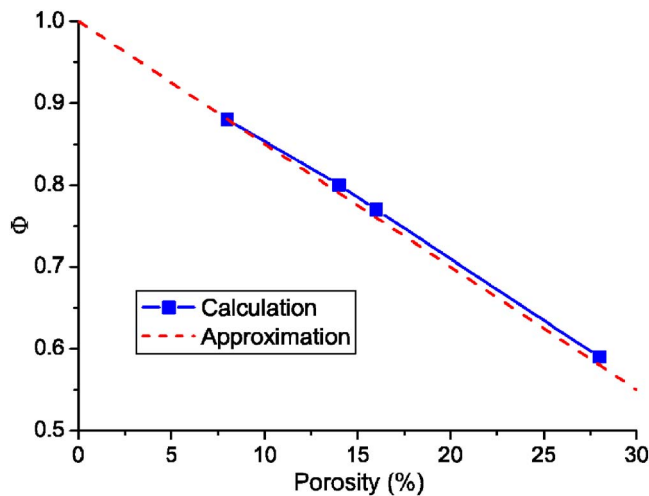


FIG. 6. (Color online) Factor of porosity for the structure in Fig. 5(a). $\kappa = \kappa_i \Phi(p)$. Dashed line corresponds to the approximation $\Phi = 1 - 3p/2$.

To estimate the effective thermal conductivity using the formalism of Sec. II, it is necessary to calculate the correlation functions of the structures in Figs. 5(a)–5(c). Such calculations have been carried out, analyzed,¹¹ and used to estimate the bounds of conductivity by Berryman.¹² In this work, we used the files of the structures, Fig. 5, in the bitmap format. We have calculated the product $\eta(r_1)\eta(r_2)$, where $\eta=0$, if the appropriate pixel is black, and $\eta=1$, if this pixel is white. The product has been averaged over an array of random points r_1 (we have used 100 000 points) of the structure for each $r=r_1-r_2$. The correlation functions W of these structures [more precisely, their projections on the r (along the plane of substrate) and z (normal to this plane)] are presented in Fig. 5 on the right from the appropriate structures.

We see that the width of the main peak of the CF of Fig. 5(a) corresponds to the size of pores, whereas additional equidistant peaks relate to the spacing between them. Similarly, the width of the central peaks of CF of Fig. 5(b) [$W(r)$ and $W(z)$] corresponds to the longer and shorter axes of the ellipses. These values can also be seen in Fig. 5(c) as different slopes of the curve for $r < 1$ and $1 < r < 4$; however, for this structure, both curves $W(r)$ and $W(z)$ coincide.

The correlation function $W(r, z)$ has been used to calculate the effective thermal conductivity $\overline{\kappa_{ij}} = \kappa_0 - \Sigma_{ij}$. In the first approximation on porosity, the correction is $\Sigma_{ij} = \Sigma \delta_{ij}$, where Σ is determined by Eq. (8) and $\tilde{W}(\mathbf{k})$ is the Fourier transform of $W(r, z)$. Corrections of the second order on porosity [$\Sigma^{(1)}$ and $\Sigma^{(2)}$] are presented by the first and second diagrams in Fig. 3, respectively. See also Eqs. (B3)–(B5) of Appendix B, where the details of calculation are presented.

The porosity of the structures in Fig. 5 is about 15%. Nevertheless, by changing the number or size of the pores, we can change the porosity. Figure 6 presents the factor of porosity Φ of the thermal conductivity of the structure of Fig. 5(a) as a function of porosity. The dashed line presents the result of the approximation $\Phi = 1 - 3p/2$, which replaces Eq. (9) in the 2D case.¹⁷ We found a good agreement even for high porosity $p \approx 30\%$.

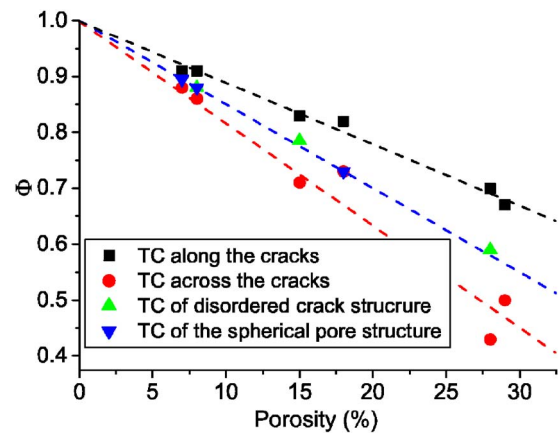


FIG. 7. (Color online) Factor of porosity for the structures from Fig. 5. $\kappa = \kappa_i \Phi(p)$. Dashed lines correspond to the approximation $\Phi = 1 - (1+J)p$, where $J=0.1$, $J=0.5$, and $J=0.8$ for the upper, central, and lower lines, respectively.

Figure 7 presents factor of porosity in the directions along and across the longer axis of the structure from Fig. 5(b). It is apparent that the thermal conductivity along the longer axis exceeds the thermal conductivity across it, and they both are appreciably distinguished from the approximation $\kappa = \kappa_i(1 - 3p/2)$. This is in agreement with Ref. 7. On the contrary, the thermal conductivity of the disordered crack structure, Fig. 5(c), is close to that of Fig. 5(a) and so to the approximation $\Phi = 1 - 3p/2$. This follows from Eq. (8) for the correlation function $\tilde{W}(\mathbf{k})$ of the cubic symmetry.

IV. THERMAL CONDUCTIVITY OF POROUS YSZ STRUCTURE

It is impossible to calculate the CF from a single 2D microscopy image of an arbitrary 3D structure. Nevertheless, sometimes this can be done using the symmetry of the structure. It seems reasonable to suppose cylindrical symmetry of thin coatings with the symmetry axis z normal to the substrate plane, so that all directions in this plane (r) are equal. Then, any microscopy image of the cut normal to the substrate plane can be used to calculate the CF $W(r, z)$.

Figure 8 presents optical micrograph of the air plasma sprayed YSZ coating and its black-and-white image. To obtain this image from the grayscale picture, we choose a threshold pixel value, i.e., we assume that the pixel is white if its value exceeds this threshold value or black otherwise. The threshold pixel value we choose ensures the pore distribution in Fig. 8(b) close to the initial, Fig. 8(a). The porosity p can then be calculated from Fig. 8(b). The threshold pixel value could also be obtained if the porosity of the structure was measured.

The correlation function, which has been obtained from Fig. 8(b) after averaging over 100 000 random points for each pair r, z from the rectangular net, is presented in Fig. 9. In comparison with the correlation functions from Fig. 5, this one is very simple, and it does not exhibit any oscillations at large distances. This is the consequence of disorder of the real coating shown in Fig. 8, which does not contain pores of

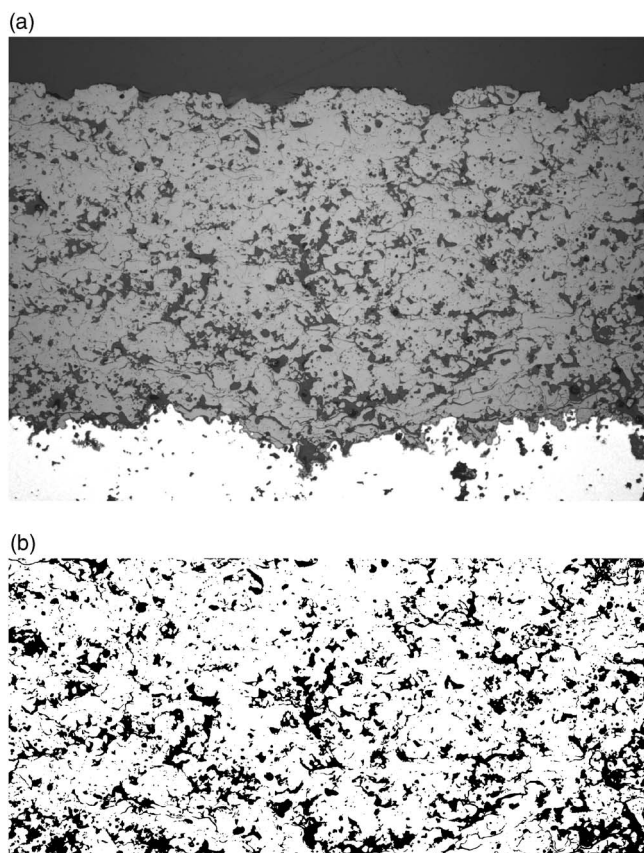


FIG. 8. (a) Optical micrograph of a 500 μm thick YSZ plasma sprayed coating and (b) its binary image.

the same shape. We found very small difference between CF in r and z directions (along and across the film plane). This means good applicability of the simple approximation $\Phi = 1 - 4p/3$. Indeed, for the coating, Fig. 8, $1 - 4p/3 = 0.69$, estimation of the porosity factor $\Phi(p)$ from diagrams of Fig. 2 yields 0.71; meanwhile, corrections coming from each diagram of Fig. 3 are 0.005 and 0.004, respectively.

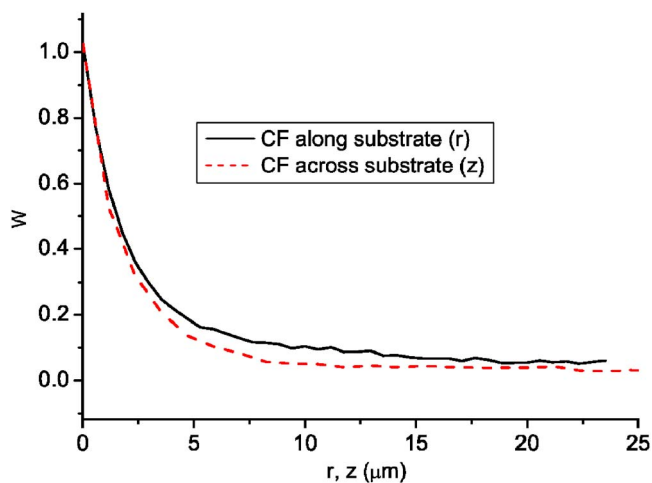


FIG. 9. (Color online) Correlation function of the coating of Fig. 8. Only its projections along and across the coating plane are shown.

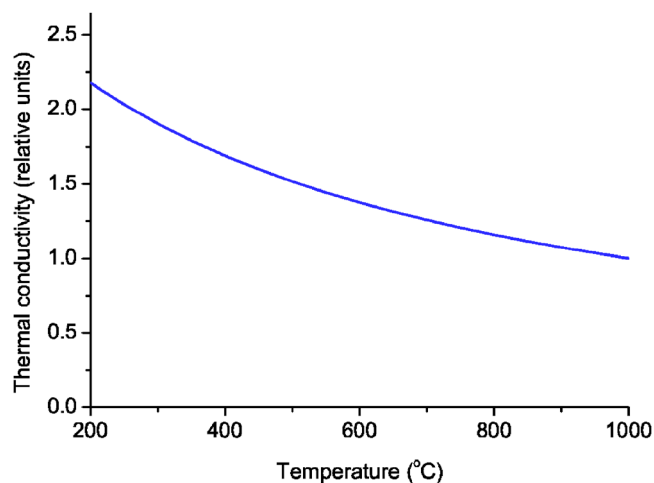


FIG. 10. (Color online) Thermal conductivity of the YSZ plasma sprayed coating shown in Fig. 8. $\kappa = \kappa_i \Phi(p)$. We adopt units where $\kappa(1000^\circ\text{C}) = 1$.

To estimate the thermal conductivity of the coating, the porosity factor $\Phi(p)$ should be multiplied by the intrinsic thermal conductivity κ_i of YSZ. We used the model of Ref. 6 to estimate κ_i as the function of temperature. The result is presented in Fig. 10.

V. DISCUSSION

To introduce the concept of effective thermal conductivity, we have considered the heat propagation from some infinitely removed point origin. This is convenient to determine the effective thermal conductivity but seems too artificial for applications. It would be more natural if we considered a thick layer of porous material assuming the average temperatures of its sides, T_1 and T_2 , to be different ($T_2 > T_1$). Then, the effective thermal conductivity could be determined by consideration of heat flux through the layer. It is not obvious that averaging the temperature or the heat flux leads to the same result. Nevertheless, such is the case: both determinations are equivalent.

Indeed, the mean heat flux across the layer is $\langle \kappa(\mathbf{r}) \text{grad } T \rangle = S^{-1} \int \kappa(\mathbf{r}) \nabla T d\sigma$, where S is the lateral area of the layer; the integration is carried out over some plane σ parallel to this area. Then, the effective thermal conductivity is

$$\bar{\kappa} = \frac{D}{T_2 - T_1} \langle \kappa(\mathbf{r}) \text{grad } T \rangle, \quad (11)$$

where D is the width of the layer.

This value of the effective thermal conductivity is equal to that determined in Sec. II. The simplest way to show that is to evaluate the mean heat flux using the diagrammatic technique developed there. To do that, we have to multiply Eq. (6) by $\kappa(\mathbf{r}) = \kappa_0 + \eta(\mathbf{r})$ and \mathbf{k}_z before averaging. The result is $\bar{\kappa} = \kappa_0 - \bar{\Sigma}$.

The identity of both determinations of thermal conductivity becomes clear, if we introduce two heat origins of opposite signs (i.e., heat source and sink) far away from the layer

(i.e., substitute $Q[\delta(-L,t) - \delta(L,t)]$ for the right part of Eq. (1)) and determine the temperatures T_1 and T_2 from Eq. (3). Then, estimation of $\bar{\kappa}$ either from Eq. (11) or from averaging of T results in the same value, because inside the layer both of them obey the same heat-flow equation,

$$\frac{\partial \bar{T}}{\partial t} - \frac{\partial^2 \bar{T}}{\partial x_i \partial x_j} = 0.$$

It seems to us that the disagreement between the factors of porosity $\Phi = 1 - 4p/3$ obtained in Ref. 5 and $\Phi = 1 - 3p/2$ obtained in Ref. 7 is due to different approaches used to calculate the averages. Note that the factor $\Phi = 1 - 3p/2$ has also been obtained in Ref. 18, where electric conductivity of porous materials has been investigated. The average electric conductivity has been estimated in Ref. 18 as $\sigma = \langle j \rangle / \langle E \rangle$, where $\langle j \rangle$ is the mean current density and $\langle E \rangle$ is the mean electric field. Our result for thermal conductivity Eq. (9) coincides with that of Ref. 5.

It should be emphasized that estimation Eq. (9) is independent of actual shape of pores; only the symmetry of the porous structure is important. Indeed, Eq. (9) follows from Eq. (8) for any correlation function $\tilde{W}(\mathbf{k})$ of cubic symmetry; therefore, it always holds in isotropic porous media of low porosity. Deviation from this law can be expected either in strongly anisotropic structures (e.g., in some plasma sprayed coatings) or in porous materials of high porosity when corrections of Fig. 3 (which are of the second order on porosity) are significant.

The correlation functions presented in Figs. 5 and 9 have one important peculiarity: their derivatives at $r=0$ are non-zero. This is the consequence of the steplike behavior of the local thermal conductivity; it is either zero (in the pores) or constant κ_i outside them. Among the one-dimensional random functions, such behavior is characteristic for the telegraph function. This function is equal to either 1 or 0, and its correlation function is $W(x) = \exp(-x/l)$, where l is the correlation length, i.e., the mean length of the step. Hence, for qualitative analysis of the porous media, we can accept the following model functions:

$$W(\mathbf{r} - \mathbf{r}') = e^{-\sqrt{(x-x')^2 + (y-y')^2 + \gamma^2(z-z')^2}/R}$$

for 3D case or

$$W(\mathbf{r} - \mathbf{r}') = e^{-\sqrt{(x-x')^2 + \gamma^2(z-z')^2}/R} \quad (12)$$

for 2D case. The dimensionless parameter γ determines the pore anisotropy. In particular, it allows investigation of spherical pores (if $\gamma=1$) or cracks directed along (for $\gamma \ll 1$) or across (for $\gamma \gg 1$) the z axis. In a certain sense, γ is similar to the λ value, which has been introduced in Ref. 8 to characterize the pore anisotropy. Unlike the commonly used Gauss correlation function, this one ensures abrupt discontinuity of the thermal conductivity at the pore boundary. The Fourier transform of Eq. (12) is

$$\tilde{W}(k, q_z) = \frac{8\pi}{\gamma R(k^2 + q_z^2 \gamma^{-2} + R^{-2})^2} \quad \text{for 3D case}$$

and

$$\tilde{W}(k, q_z) = \frac{2\pi}{\gamma R(k^2 + q_z^2 \gamma^{-2} + R^{-2})^{3/2}} \quad \text{for 2D case,} \quad (13)$$

where k and q_z are the components of the wave vector in the plane of substrate and normal to it, respectively. It is important that Eqs. (13) have power, but not exponential, factors decaying with k, q_z . This also distinguishes CF [Eqs. (12) and (13)] from the Gauss one.

Apparently, Figs. 2 and 3 represent power-series expansion of thermal conductivity as a function of porosity. To estimate the actual error due to this expansion, assume that we have a porous structure, where the pores are of the same small aspect ratio but different orientation [like that in Fig. 5(c)]. Let us write the correlation function of such structure as the sum of two exponents, Eqs. (12), with different γ parameters: W_1 and W_2 with $\gamma_1 = \gamma$ and $\gamma_2 = 1/\gamma$, respectively. By substituting $\tilde{W}_1(k_1, q_1) \tilde{W}_2(k_2, q_2)$ into Eq. (B4), we can find $\Sigma_{zz}^{(2)} \propto p^2/\gamma^2$, if $\gamma \rightarrow 0$.¹⁹ This means that contribution of the second diagram of Fig. 3 is of the order of 1, if $p^2/\gamma^2 \sim 1$, or of the order of p , if $p/\gamma^2 \sim 1$. The former condition means total demolition of the structure due to high porosity; the latter suggests that the second-order diagrams should also be taken into account. The reason is apparent: even the web of thin cracks, whose contribution to the porosity is zero, on the 2D case makes thermal conductivity vanish.

We found that the effect of second-order diagrams (Fig. 3) is very small. It is about 0.5% of the thermal conductivity for both model and real structures. This is far less than the difference between the exact upper and lower bounds of conductivity found in Refs. 11 and 12. Estimations of Refs. 11 and 12 are very useful for the structures of high porosity and small aspect ratio, if our expansion diverges because of large p/γ .

The approach we have proposed has some advantages and disadvantages. First, it permits using the microscopy image to determine the thermal conductivity of the particular specimen. Unlike approach of Ref. 9, it does not allow us to obtain the microscopical picture of the temperature or heat flux distribution. However, it allows us to distinguish rather the time-consuming routine of the image characterization (calculation of the correlation function) from the problem of thermal-conductivity estimation. The latter reduces to calculation of some integrals. Moreover, we can use a few microscopy images (obtained with different magnifications) of the same structure to calculate CF. This could be important to take into account the pores and cracks of significantly different sizes (e.g., globular and interlamellar pores in plasma sprayed YSZ coatings), which could be of equal importance for thermal conductivity. This has been shown numerically for the model two-scale structures.²⁰

The effective thermal conductivity of coatings can be written as $\bar{\kappa} = \kappa_i \Phi(p)$. The porosity factor $\Phi(p)$ depends on total porosity, the shape of pores, and their size distribution. All these factors are included into the correlation function. However, the $\Phi(p)$ factor is independent of the pore size; namely, the simultaneous increase or decrease of sizes of all pores and distances between them, which does not change the total porosity, has no effect on $\Phi(p)$. The possible depen-

dence of $\bar{\kappa}$ on the pore size, if being observed in experiments, is due to the radiation component of thermal conductivity, which has not been considered in this study.

The model we have considered here concerns the pores, whose size considerably exceeds the mean free path of phonons (or another excitation that is responsible for the heat transport); only under this condition does the heat-flow equation (4) hold. It seems possible that small size pores can also be important for thermal conductivity. This also concerns other small size structure defects, such as impurities and grain boundaries that result in the phonon scattering. In particular, this concerns phonon scattering at the grains of different polymorphic compositions that are characteristic for YSZ. Perhaps, the effect of such defects depends on the material and technology of the structure preparation. The authors of Ref. 6 showed that the phonon scattering at grain boundaries is not significant in their experiments on YSZ. On the contrary, the authors of Refs. 14 and 21 have observed essential dependence of thermal conductivity on the grain size for the same material. It seems that the disagreement between the calculated and measured values of thermal conductivity of plasma sprayed YSZ observed in the paper⁹ can be explained by the influence of the grain boundaries. To take this factor into consideration, we have to replace the intrinsic thermal conductivity κ_i with the thermal conductivity of the dense material where the phonon scattering at the grain boundaries already had been taken into account. This can be done either by the Kapitza model²¹ or by the model of Ref. 22. It has been shown³ that both models yield the same result.

In conclusion, we proposed the series expansion of the expression for effective thermal conductivity of the porous media in powers of porosity p . We found that the actual parameter of this expansion is p/γ , where γ is the aspect ratio. We showed that the coefficients of this expansion can be estimated from the microscopy image of the porous media.

ACKNOWLEDGMENT

Authors are indebted to the Innovation Promotion Agency (CTI) of the Swiss Federal Office for Professional Education and Technology (Project No. 7820.3 EPRP-IW) for financial support.

APPENDIX A: ESTIMATION OF THE EFFECTIVE THERMAL CONDUCTIVITY BY SUMMATION OF DIAGRAMS

The diagram of the second order with respect to $\tilde{\eta}$ from Fig. 1 corresponds to the expression

$$\Theta_2(\mathbf{q}) = \frac{\Theta_0(\mathbf{q})}{(2\pi)^6} \int (\mathbf{k}_1\mathbf{q})\Theta_0(\mathbf{k}_1)\tilde{\eta}(\mathbf{k}_1-\mathbf{q}) \\ \times (\mathbf{k}_2\mathbf{k}_1)\Theta_0(\mathbf{k}_2)\tilde{\eta}(\mathbf{k}_2-\mathbf{k}_1)d^3\mathbf{k}_1d^3\mathbf{k}_2.$$

This value should be averaged over $\tilde{\eta}$. Note that for the homogeneous, in average, media,

$$\overline{\tilde{\eta}(\mathbf{k})\tilde{\eta}(\mathbf{k}')} = \kappa_i^2 p(1-p) \int W(\mathbf{r}-\mathbf{r}')e^{i\mathbf{k}(\mathbf{r}-\mathbf{r}')+i(\mathbf{k}+\mathbf{k}')\mathbf{r}}d^3\mathbf{r}d^3\mathbf{r}' \\ = (2\pi)^3 \kappa_i^2 p(1-p)\tilde{W}(\mathbf{k})\delta(\mathbf{k}+\mathbf{k}').$$

Therefore,

$$\overline{\Theta_2(\mathbf{q})} = \frac{\kappa_i^2 \Theta_0^2(\mathbf{q})}{(2\pi)^3} \int [(\mathbf{q}-\mathbf{k})\cdot\mathbf{q}]^2 \tilde{W}(\mathbf{k})\Theta_0(\mathbf{q}-\mathbf{k})d^3\mathbf{k}.$$

This expression corresponds to the second diagram in the series in Fig. 2. The third diagram of this sum follows from the fourth-order diagram of the series in Fig. 1,

$$\Theta_4(\mathbf{q}) = \frac{\Theta_0(\mathbf{q})}{(2\pi)^{12}} \int (\mathbf{k}_1\mathbf{q})(\mathbf{k}_2\mathbf{k}_1)(\mathbf{k}_3\mathbf{k}_2)(\mathbf{k}_4\mathbf{k}_3)\Theta_0(\mathbf{k}_1) \\ \times \Theta_0(\mathbf{k}_2)\Theta_0(\mathbf{k}_3)\Theta_0(\mathbf{k}_4)\tilde{\eta}(\mathbf{k}_1-\mathbf{q})\tilde{\eta}(\mathbf{k}_2-\mathbf{k}_1) \\ \times \tilde{\eta}(\mathbf{k}_3-\mathbf{k}_2)\tilde{\eta}(\mathbf{k}_4-\mathbf{k}_3)d^3\mathbf{k}_1d^3\mathbf{k}_2d^3\mathbf{k}_3d^3\mathbf{k}_4,$$

and the first term (second line) of the average

$$\overline{\tilde{\eta}(\mathbf{k}_1-\mathbf{q})\tilde{\eta}(\mathbf{k}_2-\mathbf{k}_1)\tilde{\eta}(\mathbf{k}_3-\mathbf{k}_2)\tilde{\eta}(\mathbf{k}_4-\mathbf{k}_3)} \\ = \overline{\tilde{\eta}(\mathbf{k}_1-\mathbf{q})\tilde{\eta}(\mathbf{k}_2-\mathbf{k}_1)} \cdot \overline{\tilde{\eta}(\mathbf{k}_3-\mathbf{k}_2)\tilde{\eta}(\mathbf{k}_4-\mathbf{k}_3)} \\ + \overline{\tilde{\eta}(\mathbf{k}_1-\mathbf{q})\tilde{\eta}(\mathbf{k}_4-\mathbf{k}_3)} \cdot \overline{\tilde{\eta}(\mathbf{k}_2-\mathbf{k}_1)\tilde{\eta}(\mathbf{k}_3-\mathbf{k}_2)} \\ + \overline{\tilde{\eta}(\mathbf{k}_1-\mathbf{q})\tilde{\eta}(\mathbf{k}_3-\mathbf{k}_2)} \cdot \overline{\tilde{\eta}(\mathbf{k}_2-\mathbf{k}_1)\tilde{\eta}(\mathbf{k}_4-\mathbf{k}_3)}. \quad (\text{A1})$$

Two other summands of Eq. (A1) are represented by the first and second diagrams in Fig. 3.

The summation of the series, Fig. 2, leads to the calculation of the loop

$$q^2\Sigma = \frac{\kappa_i^2 p(1-p)}{(2\pi)^3} \int [(\mathbf{q}\cdot(\mathbf{q}-\mathbf{k}))]^2 \tilde{W}(\mathbf{k})\Theta_0(\mathbf{q}-\mathbf{k})d^3\mathbf{k}$$

and summation of the geometric progression. Namely, the equation represented by Fig. 2 is

$$\Theta(\mathbf{q}) = \Theta_0(\mathbf{q}) + \Theta_0(\mathbf{q})(q^2\Sigma)\Theta(\mathbf{q}),$$

i.e., $\Theta(\mathbf{q})^{-1} = \Theta_0(\mathbf{q})^{-1} - q^2\Sigma$. This results in Eq. (8).

To increase the accuracy to the second order on porosity (p^2), we have to add the diagrams in Fig. 3 to the loop Σ . This leads to the tensor correction, Eq. (10), to the loop, so that Eq. (8) accepts the form

$$\Theta = \frac{1}{(\kappa_0\delta_{ij} - \Sigma_{ij})q_i q_j - i\omega}. \quad (\text{A2})$$

The corrections higher than p^2 have not been considered in this paper; nevertheless, this could be done with the diagrammatic technique. It is important that in all these corrections, we can assume $q \rightarrow 0$, so that Σ_{ij} is independent of q . From comparison of Eq. (A2) with Eq. (2), it follows that $\kappa_{ij} = \kappa_0\delta_{ij} - \Sigma_{ij}$ is the effective thermal conductivity.

APPENDIX B: SOME FORMULAS USED IN THE CALCULATION

The Fourier transform of the correlation function

$$\tilde{W}(\mathbf{k}) = \int W(\mathbf{r})e^{i\mathbf{k}\cdot\mathbf{r}}d^3r,$$

for the 3D case of cylindrical symmetry can be simplified as

$$\tilde{W}(k, q_z) = 4\pi \int_0^\infty \int_0^\infty W(\rho, z)J_0(k\rho)\cos(q_z z)\rho d\rho dz. \quad (\text{B1})$$

For the spherical symmetry,

$$\tilde{W}(k) = \frac{4\pi}{k} \int_0^\infty W(r)r \sin(kr)dr. \quad (\text{B2})$$

Equation (B2) also follows from Eq. (B1) after the substitution $r = \sqrt{\rho^2 + z^2}$ for z and integration on ρ .

The integral, Eq. (8), for the 3D case of cylindrical symmetry reads

$$\Sigma = \frac{\kappa_i p}{2\pi^2} \int_0^\infty \int_0^\infty \frac{kq_z^2}{k^2 + q_z^2} \tilde{W}(k, q_z) dk dq_z. \quad (\text{B3})$$

For the 2D case (arbitrary symmetry),

$$\Sigma = \frac{\kappa_i p}{\pi^2} \int_0^\infty \int_0^\infty \frac{k_x^2}{k_x^2 + k_y^2} \tilde{W}(k_x, k_y) dk_x dk_y.$$

The first and second diagrams of Fig. 3 can be evaluated using the cylindrical symmetry:

$$\begin{aligned} \Sigma_{zz}^{(1)} &= \frac{\kappa_i p^2}{4(2\pi)^4(1-p)} \int \frac{k_1 k_2 q_1^2}{(k_1^2 + q_1^2)^2} I_{zz}^{(1)} \tilde{W}(k_1, q_1) \\ &\quad \times \tilde{W}(k_2, q_2) dk_1 dk_2 dq_1 dq_2, \end{aligned}$$

$$\begin{aligned} \Sigma_{zz}^{(2)} &= \frac{\kappa_i p^2}{4(2\pi)^4(1-p)} \int \frac{k_1 k_2 q_1 q_2}{(k_1^2 + q_1^2)(k_2^2 + q_2^2)} I_{zz}^{(2)} \\ &\quad \times \tilde{W}(k_1, q_1) \tilde{W}(k_2, q_2) dk_1 dk_2 dq_1 dq_2, \end{aligned}$$

where

$$I_{zz}^{(1)} = 4a_1 - A + \frac{(a_1 - a_2)^2}{\sqrt{A^2 - B^2}},$$

$$I_{zz}^{(2)} = A - \frac{(a_1 - a_2)^2}{\sqrt{A^2 - B^2}},$$

$$a_1 = k_1^2 + q_1^2 + q_1 q_2, \quad a_2 = k_2^2 + q_2^2 + q_1 q_2,$$

$$A = a_1 + a_2, \quad B = 2k_1 k_2. \quad (\text{B4})$$

In the 2D case of any symmetry, the diagrams, Fig. 3, read

$$\Sigma_{zz}^{(1)} = \frac{\kappa_i p^2}{(2\pi)^4(1-p)} \int_{-\infty}^{+\infty} \frac{q_1^2(a_1 + k_1 k_2)^2}{(k_1^2 + q_1^2)^2(A+B)}$$

$$\times \tilde{W}(k_1, q_1) \tilde{W}(k_2, q_2) dk_1 dk_2 dq_1 dq_2,$$

$$\Sigma_{xx}^{(1)} = \frac{\kappa_i p^2}{(2\pi)^4(1-p)} \int_{-\infty}^{+\infty} \frac{k_1^2(a_1 + k_1 k_2)^2}{(k_1^2 + q_1^2)^2(A+B)}$$

$$\times \tilde{W}(k_1, q_1) \tilde{W}(k_2, q_2) dk_1 dk_2 dq_1 dq_2,$$

$$\Sigma_{zz}^{(2)} = \frac{\kappa_i p^2}{(2\pi)^4(1-p)} \int_{-\infty}^{+\infty} \frac{q_1 q_2(a_1 + k_1 k_2)(a_2 + k_1 k_2)}{(k_1^2 + q_1^2)(k_2^2 + q_2^2)(A+B)}$$

$$\times \tilde{W}(k_1, q_1) \tilde{W}(k_2, q_2) dk_1 dk_2 dq_1 dq_2,$$

$$\Sigma_{xx}^{(2)} = \frac{\kappa_i p^2}{(2\pi)^4(1-p)} \int_{-\infty}^{+\infty} \frac{k_1 k_2(a_1 + k_1 k_2)(a_2 + k_1 k_2)}{(k_1^2 + q_1^2)(k_2^2 + q_2^2)(A+B)}$$

$$\times \tilde{W}(k_1, q_1) \tilde{W}(k_2, q_2) dk_1 dk_2 dq_1 dq_2. \quad (\text{B5})$$

*Electronic address: brag@isp.nsc.ru

¹R. M. Costescu, D. G. Cahill, F. H. Fabreguette, Z. A. Sechrist, and S. M. George, *Science* **303**, 989 (2004).

²D. Zhu and R. A. Miller, NASA Report No. TM-2005-213437, 2005 (unpublished); <http://gltrs.grc.nasa.gov/citations/all/tm-2005-213437.html>

³L. Braginsky, V. Shklover, H. Hofmann, and P. Bowen, *Phys. Rev. B* **70**, 134201 (2004).

⁴S. Docquir and S. Candel, *Prog. Energy Combust. Sci.* **28**, 107 (2002).

⁵P. G. Klemens, *High Temp. - High Press.* **23**, 241 (1991).

⁶K. W. Schlichting, N. P. Padture, and P. G. Klemens, *J. Mater. Sci.* **36**, 3003 (2001); P. G. Klemens and M. Gell, *Mater. Sci. Eng., A* **245**, 143 (1998).

⁷B. Shafiro and M. Kachanov, *J. Appl. Phys.* **87**, 8561 (2000).

⁸I. Sevastianov and M. Kachanov, *J. Therm. Spray Technol.* **9**, 478 (2000); *Mater. Sci. Eng., A* **297**, 235 (2001).

⁹Z. Wang, A. Kulkarni, S. Deshpande, T. Nakamura, and H. Herman, *Acta Mater.* **51**, 5319 (2003).

¹⁰P. Corson, *J. Appl. Phys.* **45**, 3159 (1974).

¹¹J. Berryman, *J. Appl. Phys.* **57**, 2374 (1984).

¹²J. Berryman, *Appl. Phys. Lett.* **86**, 032905 (2005); *J. Appl. Phys.* **97**, 063504 (2005).

¹³A. Abrikosov, L. Gor'kov, and T. Dzyaloshinskii, *Methods of Quantum Field Theory in Statistical Physics* (Dover, New York, 1975).

¹⁴G. Soyez, J. A. Eastman, L. J. Thompson, G.-R. Bai, P. M. Baldo, R. J. DiMefi, A. A. Elmustafa, M. F. Tambwe, and D. S. Stone, *Appl. Phys. Lett.* **77**, 1155 (2000).

¹⁵Equation (4) assumes zero thermal conductivity of the pores ($\kappa_p=0$). This is not always the case. To take this fact into consideration, we can reduce Eq. (4) as follows:

$$\begin{aligned} \kappa(\mathbf{r}) &= \begin{cases} \kappa_i & \text{outside the pores} \\ \kappa_p & \text{inside the pores} \end{cases} \\ &= \kappa_p + \begin{cases} \kappa_i - \kappa_p & \text{outside the pores} \\ 0 & \text{inside the pores.} \end{cases} \end{aligned}$$

Thus, we can replace everywhere κ_i with $\kappa_i - \kappa_p$ and add κ_p to the result.

¹⁶Notation *homogeneous in average porous media* means that all points in this media are equivalent, i.e., probability of some point \mathbf{r} to belong to a pore depends on total porosity, but not on the particular point \mathbf{r} . Accordingly, the average $\overline{\eta(\mathbf{r})\eta(\mathbf{r}'')}$ de-

pends on the distance $\mathbf{r}-\mathbf{r}'$, but not on \mathbf{r} . This allows us to calculate this average from the single microscopy image by summation of $\eta(\mathbf{r})\eta(\mathbf{r}'')$ taken at different points \mathbf{r} for the same $\mathbf{r}-\mathbf{r}'$.

¹⁷Note that for the 2D case, $\Sigma = p\kappa_i/2$, so that $\bar{\kappa} = \kappa_i(1-3p/2)$.

¹⁸S. Torquato, *Random Heterogeneous Materials: Microstructure and Macroscopic Properties* (Springer, New York, 2002).

¹⁹This estimation comes from the regions of small k_1, k_2, q_1 , and q_2 in the integrand Eq. (B4).

²⁰H.-F. Zhang, X.-S. Ge, and H. Ye, *Appl. Phys. Lett.* **89**, 081908 (2006).

²¹Ho-Soon Yang, G.-R. Bai, L. J. Thompson, and J. A. Eastman, *Acta Mater.* **50**, 2309 (2002).

²²L. Braginsky, N. Lukzen, V. Shklover, and H. Hofmann, *Phys. Rev. B* **66**, 134203 (2002).